

# A 2-GeV, 1-MW PULSED PROTON SOURCE FOR A SPALLATION SOURCE\*

Y. Cho, Y.-C. Chae, E. Crosbie, H. Friedsam, D. Horan, R. Kustom, E. Lessner, W. McDowell,  
D. McGhee, H. Moe, R. Nielsen, G. Norek, K. Peterson, K. Thompson, M. White

Argonne National Laboratory, Argonne, IL 60439 USA

## ABSTRACT

A design study of a 1-MW pulsed proton source based on a 2-GeV rapid cycling synchrotron (RCS) has been completed. The RCS operates at a 30-Hz repetition rate. A 400-MeV  $H^-$  injector linac allows transverse phase-space painting during injection. The linac beam is chopped near the ion source so that the phase-space of the incoming beam fits into the waiting synchrotron bucket. Chopping in this way minimizes potential beam loss during the rf capture process. An rf system provides a peak voltage of about 180 kV with a frequency swing of 1.1 to 1.5 MHz. The rf voltage programming was developed using particle tracking that included space-charge effects, in order to eliminate possible beam losses. The design takes into account re-use of existing buildings and infrastructure of the former 12-GeV Zero Gradient Synchrotron.

## 1 INTRODUCTION

A feasibility study for upgrading the Intense Pulsed Neutron Source (IPNS) at Argonne National Laboratory has been completed [1]. The 1-MW spallation source is based on a proton synchrotron that accelerates the 400-MeV linac beam to 2 GeV and delivers  $1.04 \times 10^{14}$  protons per pulse at a repetition rate of 30 Hz. The choice of 30 Hz as the repetition rate was based on preferences expressed by the neutron community. Full power can be delivered to a 30-Hz target station or one out of three pulses to a 10-Hz station and the remaining two pulses to the high-frequency station. The synchrotron system and associated research facilities are housed in the former 12-GeV Zero Gradient Synchrotron (ZGS) area and occupy about 50,000 m<sup>2</sup>. The 190-m, 2-GeV RCS is housed in the ZGS tunnel and the two neutron-producing targets, each serving 18 neutron beamlines, are placed in former experimental area buildings. Enclosures for the linac and low energy transport line (LET) are the only new conventional facility construction.

## 2 LATTICE

The lattice design provides: a) a large transition energy so that the lattice has a relatively large slip factor,  $\eta = |\gamma^{-2} - \gamma_t^{-2}|$ , b) enough straight-section length for a radio-frequency cavity system that could have a total

length of 20-30 m, and c) dispersion-free straight sections for implementation of charge-exchange injection. Figure 1 shows 1/2 of a superperiod with reflective symmetry at both ends. Each cell of the FODO structure has a phase advance of  $\sim 90^\circ$  in both transverse planes. The normal cells, dispersion-suppressor cell and the straight-section cells are evident in the figure. The dispersion-suppressor cell is made by removing a dipole from a  $90^\circ$  phase advance cell. The vertical phase advance is slightly less than  $90^\circ$  but the horizontal phase advance is maintained at  $90^\circ$ , so that the missing dipole scheme effectively suppresses the dispersion function. An advantage of this arrangement is that the horizontal tune is about one unit higher than the vertical. Taking alignment and construction imperfections into account, tracking studies showed that the RCS has a dynamic aperture larger than the physical aperture of the ring vacuum chamber [2]. Table 1 is a summary of the main RCS parameters.

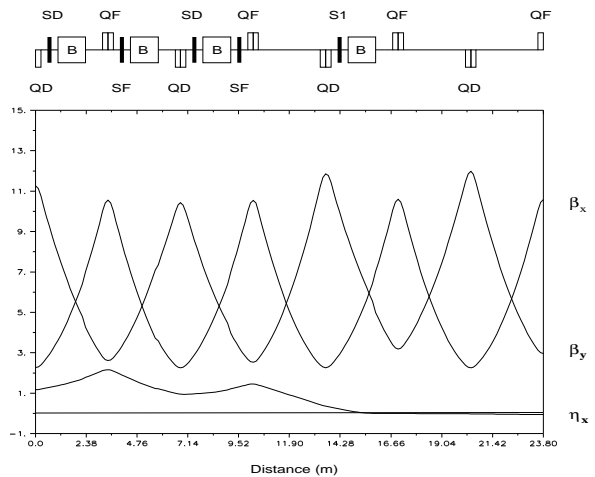


Figure 1: Lattice functions for 1/2 superperiod.

## 3 INJECTION

The injection energy was determined by the incoherent space-charge limit of the lattice and the defined acceptance of the synchrotron. The injected beam stack has an emittance of  $375 \pi$  mm mr in both transverse planes. With a bunching factor of 0.4 and an allowed tune shift due to space-charge of 0.15, an injection energy of 400 MeV is sufficient to provide a time-averaged current of 0.5 mA with a repetition rate of 30 Hz.

The 400-MeV  $H^-$  ion injector linac design for this feasibility study was performed by the industrial firm

\* Work supported by the U.S. Department of Energy, Office of Basic Energy Sciences under Contract W-31-109-ENG-38.

AccSys Technology, Inc. The linac design specifications include: 1) an rms normalized emittance of  $1 \pi \text{ mm mr}$ , 2) an energy spread of less than 2.5 MeV, 3) a beam pulse length of 0.5 ms, and 4) beam-chopping capability near the ion source so that the beam can be injected into a waiting synchrotron rf bucket.

**Table 1:** Main Parameters of the RCS.

Parameters	Values	Units
Circumference	190.4	m
Super-periodicity	4	-
Total number of cells	28	-
No. of normal cells	12	-
No. of dispersion-suppressor cells	8	-
No. of straight-section cells	8	-
Nominal straight-section length	2.9	m
Injection energy	400	MeV
Injection field	0.463	T
Nom. extraction energy	2.0	GeV
Maximum design energy	2.2	GeV
Dipole field at 2.0 GeV	1.4029	T
Bending radius	6.621	m
Dipole length	1.3	m
Quadrupole length	0.5	m
Maximum quad. gradient	8.8	T/m
Maximum sextupole strength	1.2	$\text{m}^{-2}$
Sextupole length	0.2	m
Horizontal tune, $\nu_x$	6.821	-
Vertical tune, $\nu_y$	5.731	-
Normal. trans. energy, $\gamma_t$	5.40	-
Natural chromaticity, $\xi_x=(\Delta\nu)_x/(\Delta p/p)$	-7.23	-
Natural chromaticity, $\xi_y=(\Delta\nu)_y/(\Delta p/p)$	-6.88	-
Maximum $\beta$ function	12	m
Minimum $\beta$ function	2.2	m
Maximum $\eta$ function	2.2	m
Minimum $\eta$ function	-0.06	m
Rev. period at injection	890.1	ns
Rev. period at extraction	665.1	ns
$\dot{B}_{\text{max}}$	64.5	T/s
Max. energy gain/turn	81.4	keV

Phase-space painting in both transverse planes is used to stack 561 turns in the synchrotron. Four bumper magnets provide radial closed-orbit displacement, and both injection position and angle can be radially adjusted. A fast vertical steering magnet allows adjustment of the vertical injection angle. Unique features of this injection system include: 1) Trajectories of incoming  $\text{H}^-$  ions and circulating protons are combined by one of the ring focusing quadrupole magnets rather than by the customary dipole magnets. This focusing quadrupole has the added advantage that it acts as a defocusing quadrupole for the incoming  $\text{H}^-$  beam, and it provides an additional bend for the  $\text{H}^-$  particles. There is ample separation between the incoming beam and the circulating beam. 2) Since each cell has  $90^\circ$  phase advance, two bumper magnets can

displace and restore the closed orbit. However, two additional magnets are needed to adjust the injection angle of the  $\text{H}^-$  ions so that  $\text{H}^0$  particles emerging from the stripping foil can be collected in a catcher. A discussion of the  $\text{H}^-$  and  $\text{H}^0$  particles associated with this injection system is given in reference [3]. Using the bumper system together with the vertical steering magnet in the transport line, the injected beam can be stacked in a Kapchinskij-Vladimirskij (K-V) distribution [4].

## 4 RF AND THE RF VOLTAGE PROGRAM

The RCS rf system has 10 single-ended ferrite-loaded cavities to generate the required 180 kV. There is one cavity per straight section and a total of ten straight sections dedicated for the installation of the cavities. A change in resonant frequency from 1.12 MHz at injection to 1.50 MHz at extraction is accomplished by changing the dc current in the bias windings that are wound around the ferrite.

A key goal of the design study was to devise an rf program that prevents beam loss from injection through acceleration to extraction. The rf program was obtained using a Monte Carlo program that tracked the particles from injection to extraction. The tracking study also provided information on optimum chopping of the incoming beam. The beam is chopped by 25% to prevent losses and to provide sufficient energy spread to maintain the beam above the microwave instability threshold. Figure 2 shows the rf voltage program and the corresponding bucket and bunch areas. When the first turn arrives at the start of injection, the voltage required to contain the 2.5 MeV energy spread of the linac beam is 40 kV. The injected beam has a bunch area of 3.3 eV s, and the waiting bucket has an area of 7.3 eV s, thus the initial dilution of the area is a factor of 2.2. During injection the voltage is raised to 69 kV to compensate for space-charge effects and to give a slightly larger bucket area of 9 eV s.

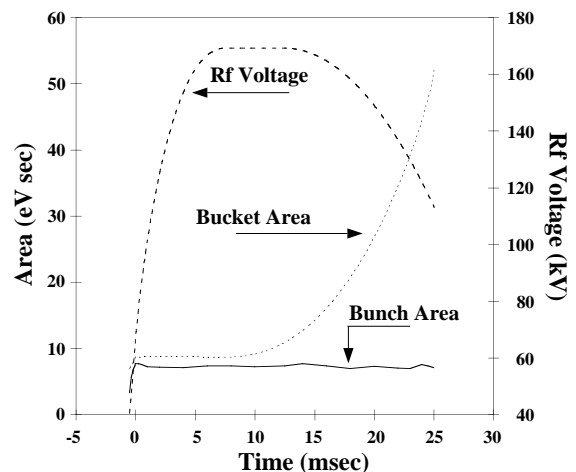


**Figure 2:** The rf voltage program, showing bunch and bucket areas over the complete cycle.

Soon after injection, the bunch is well formed. The 9 eV s bucket area is maintained for the next 7.5 ms. The

bucket area beyond that point in time is made larger, as indicated in Figure 2, for two reasons. The first is to make the momentum spread of the circulating beam large enough to stay below instability thresholds [5,6], and the second is to provide a synchrotron frequency large enough so that the particles in the bunch can follow the rapidly changing synchronous phase angle near the time of extraction.

## 5 IMPEDANCES AND INSTABILITIES

The potential excitation of intensity-dependent collective instabilities in the RCS is controlled by: a) minimizing the machine impedance by using a contour-following rf shield, and b) maximizing the tune spread to make use of Landau damping. Longitudinal and transverse instability thresholds were obtained from the estimated coupling impedances, which are dominated by space-charge effects. Beam parameters such as  $\Delta p/p$  and peak current were obtained through Monte Carlo studies of beam capture and acceleration.

The ceramic vacuum chamber is constructed with a special rf shield, similar to that used at the ISIS facility of Rutherford-Appleton Laboratory [7], to minimize the impedance due to space-charge. The shield follows the beam envelope at an aperture equal to the beam-stay-clear (BSC) and reduces both the longitudinal and transverse space-charge impedances by about 35% at injection.

The RCS operates below the transition energy, thus the longitudinal microwave instability is not expected to occur unless there is a large resistive impedance component. A conservative approach was adopted to prevent the onset of longitudinal microwave instability by ensuring that the momentum spread is sufficient to satisfy the Keil-Schnell stability criterion, modified for bunched beams. The time-variation of the momentum spread corresponding to the threshold for the microwave instability is plotted in Figure 3 together with the momentum spread obtained from the simulation. The beam remains in the stable region through the cycle.

The head-tail effect and transverse microwave instability were analyzed in detail. The head-tail modes are stabilized at a slightly negative chromaticity. The threshold tune spread for transverse microwave instability is 0.06. Stability is achievable either by choosing a chromaticity between the natural value and zero or by adding octupoles, while at the same time ensuring that the tune spread remains inside a resonance-free working region and the dynamic aperture is adequate.

## 6 SUMMARY

The accelerator system for the IPNS Upgrade is capable of delivering 1 MW of proton beam power. Full power can be delivered to a 30-Hz neutron-generating target or can be split between a 30-Hz and a 10-Hz target. A total of  $1.04 \times 10^{14}$  particles are injected into the RCS by charge-exchange injection and a phase-space-painting scheme that determines a K-V distribution. The design goal of low losses during injection, capture, and acceleration is achieved by providing a large dynamic

aperture in the transverse plane and sufficient bucket area in the longitudinal plane.

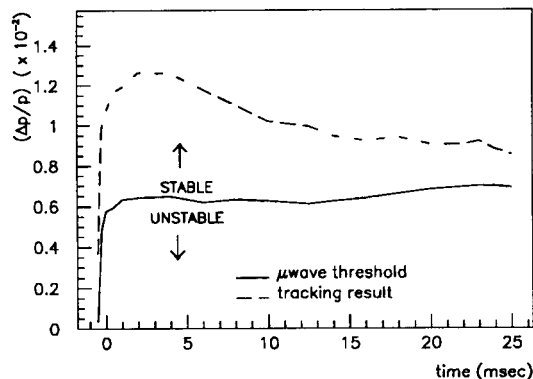


**Figure 3:** Threshold  $\Delta p/p$  compared to that obtained from tracking. The small variations are due to the Monte Carlo statistics.

## ACKNOWLEDGMENTS

We acknowledge the contributions of K. Harkay in performing the impedance and instability calculations.

## REFERENCES

- [1] "IPNS Upgrade - A Feasibility Study," ANL Report ANL-95/13 (April, 1995).
- [2] E. Lessner, Y.-C. Chae, and S. Kim, "Effects of Imperfections on Dynamic Aperture and Closed Orbit of the IPNS Upgrade Synchrotron," Proceedings of the 1995 Particle Accelerator Conference, Dallas, Texas, May 1995, p. 2811 (1996).
- [3] Y.-C. Chae and Y. Cho, "Study of Field Ionization in Charge Exchange Injection for the IPNS Upgrade," Proceedings of the 1995 Particle Accelerator Conference, Dallas, Texas, May 1995, p. 3412 (1996).
- [4] E. Crosbie and K. Symon, "Injecting a Kapchinskij-Vladimirskij Distribution into a Proton Synchrotron," Proceedings of the 1995 Particle Accelerator Conference, Dallas, Texas, May 1995, p. 3167 (1996).
- [5] K. Harkay, Y. Cho, and E. Lessner, "Longitudinal In-stability Analysis for the IPNS Upgrade," Proceedings of the 1995 Particle Accelerator Conference, Dallas, Texas, May 1995, p. 3001 (1996).
- [6] K. Harkay and Y. Cho, "Transverse Instabilities Analysis for the IPNS Upgrade," Proceedings of the 1995 Particle Accelerator Conference, Dallas, Texas, May 1995, p. 3004 (1996).
- [7] G. H. Rees, "Status Report on ISIS," Proceedings of the IEEE Particle Accelerator Conference, March 1987, p. 830 (1987).